Experimental evaluation of thermal performance and entropy generation inside a twisted U-tube equipped with twisted-tape inserts

A. Feizabadi[a], M. Khoshvaght-Aliabadi[b],*, Asghar B. Rahimi[a],**

[a] Department of Mechanical Engineering, Faculty of Engineering, Ferdowsi University of Mashhad, Mashhad, Iran
[b] Department of Chemical Engineering, Shahrood Branch, Islamic Azad University, Shahrood, 36199-43189, Iran

ABSTRACT

In this experimental study, hydrothermal characteristics of a U-tube equipped with twisted-tape inserts are investigated experimentally. The twisting effects of side wall are also investigated for the U-tube as compared to the smooth case. Two twist ratios of 2 and 6 are considered for the twisted-tape and tested in both the smooth and the twisted U-tube at the turbulent flow regime ($3843 < Re < 11{,}436$). In order to provide a condition close to uniform wall temperature, the test sections are immersed in the isothermal external fluid. The obtained results show an ascending trend for both the Nusselt number and the friction factor as the twist ratio is decreased. It is found that decreasing the twist ratio decreases the entropy generated by heat transfer and increases the entropy generated by friction loss. In the twisted U-tube fitted with the twisted-tape, the highest augmentations of 122.4% and 78.4% are recorded for Nusselt number and friction factor as compared to the smooth U-tube. The non-dimensional entropy generated by heat transfer governs the magnitude order of the non-dimensional total entropy generation. The entropy generation values of the enhanced models range between 0.63 and 1.09.

1. Introduction

Over the last decade, energy-saving concerns have gained momentum partly in response to the alarming increase in global demand for energy, the high costs associated with the production and distribution of energy, and the limited energy sources available, thus triggering an increase in the number of studies on effective methods to improve the performance of thermal systems. Heat transfer processes can be enhanced through active and passive approaches, both being widely implemented to increase the heat transfer coefficient in all areas of engineering and industries including refrigeration, air conditioning, heat recovery, solar heating, chemical reactors, electronic cooling, and the like [1]. Passive approaches are generally based on surface treatment, generating swirl flow with fluid turbulators (such as the curved tube, twisted-tape inserts, and twisted tube), and the employment of additives in working fluid [2].

In all of the currently used enhancers, the incorporation of twisted-tape inserts is one of the most favorable techniques used to enhance heat transfer in heat exchangers, which has attracted great attention compared to other passive methods partly due to the ease associated

with its generation and installation, the low costs involved, and other apparent benefits [3]. Comprehensively, the mechanism analysis concerning the heat transfer enhancement of tube with inserts have been studied based on the physical quantity synergy analysis [4–6]. In fact, such enhancers make the thermal/hydrodynamic layer smaller along the flow path, hence with higher heat transfer coefficient [7].

Experimental evaluation of thermal performance inside a tube using cross hollow twisted tape inserts was conducted by He et al. [8]. It was revealed that the cross hollow twisted tape inserts have better efficiency under laminar flow relative to turbulent flow. Eiamsa-ard et al. [9] experimentally analyzed the effect of twin twisted tapes on hydrothermal characteristics for turbulent regime. They pointed out that the twin counter twisted tapes showed better thermal performance relative to the twin co-twisted tapes. Abolarin et al. [10] examined the effect of alternating clockwise and counter clockwise twisted tape and connection angle on the hydrothermal characteristics and discovered that heat transfer improved as the connection angle was increased. Eiamsa-ard and Kiatkittipong [11] experimentally and numerically worked on different arrangement of multiple twisted tape inserts and found that the effect of multiple twisted tape inserts compared to plain tube and

* Corresponding author.
** Corresponding author.
E-mail addresses: mkhaliabadi@gmail.com, mkhaliabadi@iau-shahrood.ac.ir (M. Khoshvaght-Aliabadi), rahimiab@um.ac.ir, rahimiab@yahoo.com (A.B. Rahimi).

single twisted tape insert on heat transfer were significant. Guo et al. [12] introduced the new design of short-width and center-cleared twisted-tapes. They reported that by decreasing the gap between the edge of tape and inner diameter, the heat transfer rate decreased, while the heat transfer was strengthen with a suitable central clearance ratio. Zhang et al. [13] performed a numerical analysis to evaluate the influence of triple and quadruple twisted tapes on hydrothermal characteristics. They pointed out that the Nusselt number of tube with triple and quadruple twisted tapes possessed the maximum increment of 171% and 182%, respectively. The effect of the perforation diameter ratio on flow characteristics and heat transfer inside a tube using perforated twisted tapes experimentally evaluated by Thianpong et al. [14]. It was found that the thermal performance and frictional resistance increased as the hole diameter ratio was decreased. Qi et al. [15] analyzed the intensification of heat transfer in nanofluid flow through different structure of twisted tapes in a tube with a triangular cross section. It was found that heat transfer coefficient increased up to around 52.5% and 34.7% in laminar and turbulent regime, respectively. Meyer and Abolarin [16] made an experimental investigation to evaluate the effects of different twist ratios and heat flux in transitional flow. They reported that at a given heat flux, the transition began earlier with the increment in the twist ratio. The effect of spiky twisted tapes and nanofluid on flow resistance and heat transfer in a U-tube heat exchanger was studied by Khoshvaght-Aliabadi et al. [17]. The experimental results indicated that using spiky twisted tapes enhanced the heat transfer about 11–67%. Turbulent flow and heat transfer inside a double pipe U-bend fitted with twisted tape inserts in presence of Fe_3O_4 nanofluid experimentally was examined by Kumar et al. [18]. It was revealed that installation of twisted tapes led to the heat transfer rate increased about 38.75%.

It seems that the thermal performance of an enhancer can be improved through implementation of twisted tube along with twisted-tape inserts. In the 1980s, twisted tubes were generated by the forming of noncircular tubes [19]. There have been, however, a dearth of research studies on the hydrothermal performance of twisted tubes [20–26]. However, some researchers attempted to conduct investigations on hydrothermal characteristics through the enhanced tubes using twisted-tape [27–30]. The effect of change in the ratio of width of triple-channel twisted tape to hydraulic diameter of three-start spirally twisted tube on thermal performance was numerically examined by Eiamsa-ard et al. [27]. They discovered that the overall thermal performance increased as this parameter was increased. Hong et al. [28] experimentally analyzed the behavior of heat transfer inside a spiral grooved tube using twin twisted tapes. The results showed that the combination of spiral grooved tube and twisted tapes improved the overall performance at low Reynolds number. Hemmat Esfe et al. [29] evaluated the influence of pitch ratio on the hydrothermal characteristics of a tri-lobed tube in turbulent flow. It was found that heat transfer rate and frictional resistance enhanced as pitch ratio was increased. Hong et al. [30] made numerical analysis to examine the multiple twisted tapes effect in thermal performance of sinusoidal rib tube (SRT) heat exchangers. Their results indicated that the SRT using multiple twisted tapes possessed heat transfer rate of 1.43–1.87 times higher in comparison with SRT without twisted tape.

Moreover, the evaluation of heat transfer enhancement methods through the second law of thermodynamics are receiving more attention. Bejan discussed this analysis in more detail [31,32].

Zheng et al. [33] analyzed the effect of inclined grooves on entropy generation and reported that the entropy generation rate decreased with a reduction in the groove pitch ratio, and with a rise in the number of circumferential grooves. Kotcioglu et al. [34] evaluated the influence of a new winglet-type vortex generator in a pipe with respect to the entropy generation minimization method. The impacts of alternation made in design factors of coiled wire turbulators in a circular tube on entropy generation analyzed experimentally by Keklikcioglu and Ozceyhan [35]. They pointed out that coiled wire turbulators were

efficient up to about 10000 Reynolds number in terms of entropy generation. The twisted tape insert effect in three start spirally corrugated tubes on entropy generation were analyzed experimentally by Zimparov [36]. Sheikholeslami et al. [37] analyzed the behavior of nanofluid turbulent flow in a circular duct using modified turbulators from the second law of thermodynamics and exergy loss viewpoint. It was concluded that exergy loss enhanced by decreasing the Reynolds number and revolution angle. Rashidi et al. [38] made a numerical analysis on the impacts of eccentricity on entropy generation and hydrothermal characteristics in a tube using helical screw tape insert. They explained that the entropy generation increased with the increment in the eccentricity, especially in the region next to the tube wall. In another investigation, Sheikholeslami et al. [39] numerically simulated the behavior of nanofluid flow in a pipe using twisted-tape turbulators in terms of entropy generation. The potential influence of varying values of pitch ratio and Reynolds number was examined. It was found that Bejan number enhanced by increasing the pitch ratio, while this parameter showed a decreasing trend when Reynolds number was increased. Li et al. [40] also reported similar results in their research work on entropy generation of a heat exchanger using helically twisted tape. Mwesigye et al. [41] made a numerical analysis of the wall-detached twisted-tape effect on hydrothermal characteristics and entropy generation in a parabolic trough receiver. It was shown that for each twist ratio and width ratio, being a Reynolds number that the entropy generation rate is reduced to the least possible value. Also, it was detected that with reduction in width ratios and the increment of twist ratio was associated with the optimal Reynolds number increased. Hong et al. [42] experimentally evaluated the impact of overlapped multiple twisted-tape inserts on entropy generation and hydrothermal characteristics. The observation revealed that both reducing overlapped twist ratio and increasing tape number led to thermal irreversibility decreased while increased the frictional irreversibility. Bahiraei et al. [43] numerically examined the behavior of hybrid nanofluid flow in a pipe using double twisted-tape in terms of entropy generation. It was detected that counter twisted tapes relative to co-twisted tapes provided lower entropy generation rate.

The review of the literature shows that several passive techniques and the combination of them have been utilized so far to assess the hydrothermal performance and entropy generation rate, but there is no available study dealing with twisted-tape insert applications inside twisted U-tube. In this study, firstly, the potential of twisted-tapes on hydrothermal characteristics of twisted U-tube is investigated, then, to identify the best model and condition, the entropy generation minimization method is utilized.

2. Details of experimental system

2.1. Setup

Experiments are conducted in a fabricated setup, which is schematically shown in Fig. 1. It comprises two closed units: unit No. 1 and unit No. 2. The unit No. 1 is the main section in the present experiments, and the cooling process is performed by unit No. 2.

In the first part of the unit No. 1, the process of working fluid transmission is carried out. Water as working fluid is continuously transmitted from a reservoir (stainless steel) to principal pipe by a centrifugal pump (PKm60, Pedrollo), and the flow rate is regulated through a needle valve (LMC, ASC.15). In the second part, the process of measuring some important characteristics, including volumetric flow rate, temperature, and pressure is performed. The flow rate is gauged by a sensitive ultrasonic flow meter (Flownetix® 100 series™) with an accuracy of $\pm\,0.8 \mathrm{e}^{-07}\,\mathrm{m}^3/\mathrm{s}$. Two calming sections with 1 mm length are supplied before and after the test chamber, and two transmitters (PSCH0.5BCIA, Sensys) and two thermocouples (T-type) are located at these sections to measure the inlet/outlet pressures and temperatures. These instruments are accurate to $\pm\,10\,\mathrm{Pa}$ and $\pm\,0.1\,\mathrm{K}$. It should be
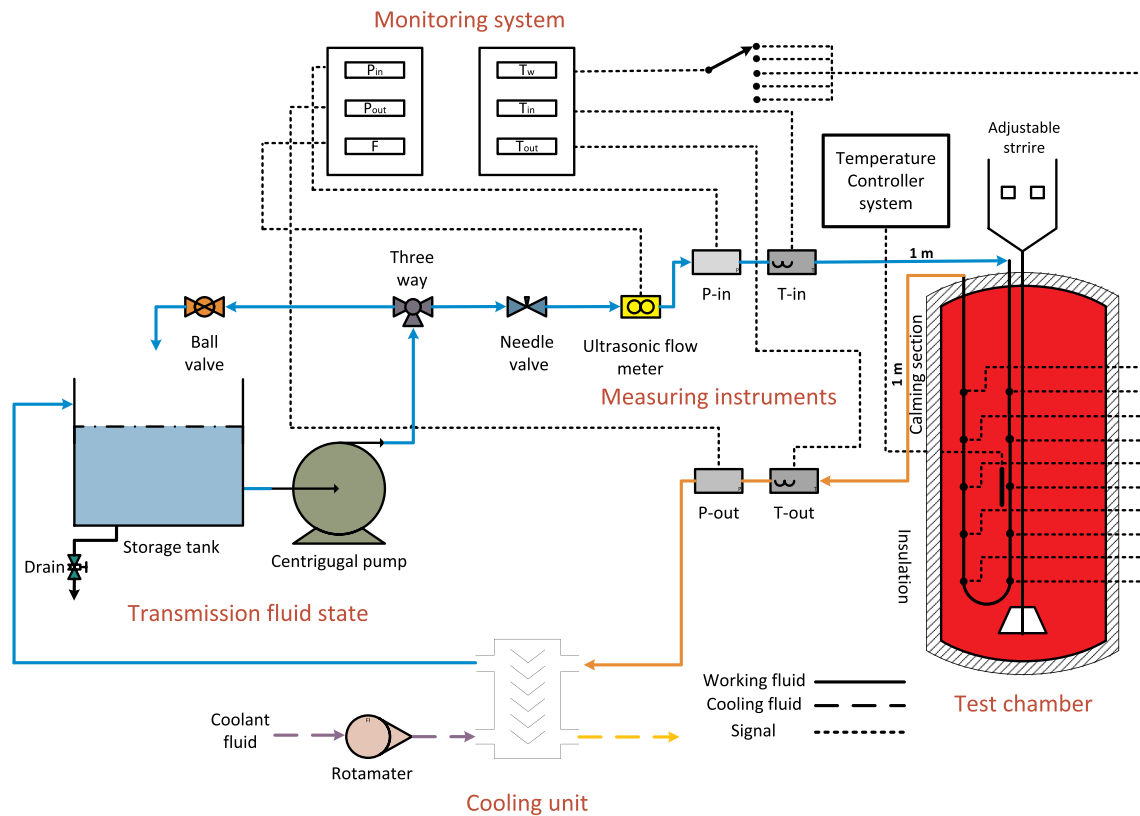
Fig. 1. A schematic representation of the experimental facilities.

noted that there is not any valves or elbows between the calming sections and the U-tube.

The cooling process of the output hot water from the test chamber is carried out by the unit No. 2 containing a polycarbonate coolant fluid tank, a centrifugal pump (PKm60, Pedrollo), a rotameter (LZT- 1005G, MBLD), a plate heat exchanger (B3-014C-12-3.0-H, Danfuss), and a refrigerator system. The cooling fluid (ethylene-glycol) is derived to the plate heat exchanger by the centrifugal pump, and the rate of coolant fluid is regulated by the rotameter. In the plate heat exchanger, the coolant fluid absorbs heat from the working fluid (water), leading to restore the temperature of water to the inlet condition (298.15 K). More details about the experimental setup are avoided due to space limitation concerns here but are provided in Refs. [44,45].

2.2. Test chamber and twisted-tape characteristics

In this section, a brief description of the test chamber along with the characteristics of U-tubes and twisted-tapes is presented. As shown in Fig. 1, it can be observed that the test chamber is an agitated heat exchanger containing a cylindrical vessel (stainless steel), an electric stirrer (RZR 2021, Heidolph), four electrical heaters (U-shape, 1000 W), a U-tube as a flow passage of water, a temperature controller system to adjust the temperature of the vessel liquid, and ten surface thermocouples (K-type), which are attached at five points on the wall surface of the U-tube with a 0.09 m uniform space to measure the surface temperatures. This is done by drilling a very small pilot hole into the tube and securing the thermocouple with a drop of solder. EPDM and glass wool are used for insulating the cylindrical vessel to avoid the dissipation of energy. In the current study, two configurations, i.e. smooth and twisted, are considered for the U-tube immersed in shell side liquid. Firstly, the hydrothermal characteristics of the heat exchanger are investigated for both configurations without inserts. Then, the experiment is repeated, with the twisted-tapes inserted inside them to augment the heat transfer. The U-tubes are fabricated of straight

copper tubes with inner diameter, thickness, and length of 15.2 mm, 1 mm, and 1000 mm, respectively. The twisted-tapes are fabricated of stainless-steel sheets with width and thickness of 15 mm and 1 mm, respectively. The clearance between the width of tapes and the inner diameter of tubes is 0.1 mm, which creates the required space for adjusting the twisted-tapes in the U-tubes. Full details of geometrical parameters are summarized in Table 1.

The twist ratio is expressed as the proportion of the length that is rotated 180° to the width of tube or tape. In the current study, the twist ratio of the twisted tube is considered constant (0.65), while two values are considered for the twisted-tapes (2 and 6). The photograph and six different layouts of twisted-tapes and U-tubes for convenient view are shown in Figs. 2 and 3.

2.3. Procedure

The following experimental procedure is executed:

Table 1
The details about geometrical parameters.

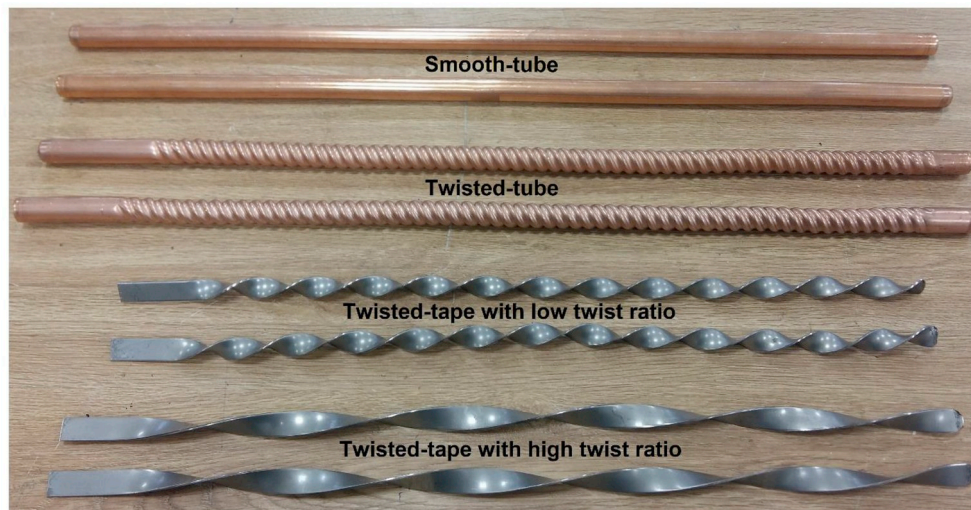| Test section	
Inner tube diameter, D	15.2 mm
Outer tube diameter	17.2 mm
Tube thickness, t	1 mm
Pitch of U-bend	50 mm
Tube length, L	1000 mm
Twist length, y	10 mm
Twist ratio, y/D	0.65
Test tube material	Copper
Twisted tape	
Twist length, y	30 and 90 mm
Tape width, w	15 mm
Tape thick, δ	1 mm
Twist ratio, y/w	2 and 6
Tape material	Aluminum

Fig. 2. Fabricated twisted-tube and twisted-tapes.

1. The reservoirs of U-tube side and shell side are filled with particular volumes of water.
2. The stirrer is switched on and regulated at the desired speed.
3. The centrifugal pump is turned on, and the rate of flow is arranged at the desired value and fluid is allowed to flow for few minutes.
4. The temperature of the shell side is controlled using the temperature controller system.
5. The outlet temperature of the water is restituted using the cooling unit to reach the initial value.
6. The changes in ten temperature sensors mounded on surface are monitored until constant value is achieved for approximately 30–40 min at each operation.
7. After the steady-state condition, the required data are logged.
8. The water flow rate is raised; afterward, the steps (5) and (7) are repeated.
9. Step (8) is repeated until the greatest value of the flow rate is achieved.

3. Data reduction

3.1. Hydrothermal characteristics

During the tests, the temperature controller system maintains the temperature of the vessel liquid at the constant value (T_e = 308.15 k). The U-tube as a flow passage of water absorbs heat through the vessel liquid. The heat transferred from the shell side liquid is described by,

$$Q_{conv} = \rho V C_p (T_{b,out} - T_{b,in}) \tag{1}$$

The internal heat transfer coefficient is predicted by Newton's law,

$$h = \frac{Q_{conv}}{A_{conv}(T_w - T_b)_{LMTD}} \tag{2}$$

where

$$(T_w - T_b)_{LMTD} = \frac{\Delta T_{w-b,in} - \Delta T_{w-b,out}}{Ln(\Delta T_{w-b,in}/\Delta T_{w-b,out})} \tag{3}$$

The following relation is used to compute the mean wall temperature along the tube side,

$$T_w = \frac{1}{10} \sum_{i=1}^{10} T_{wi} \tag{4}$$

where T_{wi} is the temperature measured by a surface thermocouple at a particular point along the tube side length.

The internal Nusselt number over tube is expressed as follows,

$$Nu = \frac{hD_h}{\kappa} \tag{5}$$

where the tube hydraulic diameter is,

$$D_h = \frac{4A_c}{P_w} \tag{6}$$

For both the smooth and the twisted U-tubes without twisted-tape,

$$A_c = \frac{\pi D^2}{4} \tag{7}$$

For both the smooth and the twisted U-tubes with twisted-tape,

$$A_c = \frac{\pi D^2}{4} - w\delta \tag{8}$$

Also, The Reynolds number is written by,

$$Re = \frac{\rho u D_h}{\mu} \tag{9}$$

The pressure drop can be measured from the values observed at the upstream and downstream of the calming sections, and is determined by using the following relation,

$$\Delta p = p_{in} - p_{out} \tag{10}$$

The pressure drop values are used for evaluation of friction factor as below [46],

$$f = \frac{2D_h \Delta p}{l\rho u^2} \tag{11}$$

To investigate the efficacy of two passive techniques implemented in the present study, the comparison between the overall performance of the tested twisted U-tube with twisted-tapes and the primary model is obligatory. The overall performance evaluation criterion or the surface goodness factor is defined as [47],

$$JF = \frac{(Nu_{Enh}/Nu_{ST})}{(f_{Enh}/f_{ST})^{1/3}} \tag{12}$$

3.2. Entropy generation analysis

Here, the theoretical formula of entropy generated in circular duct drowned in shell side with an isothermal liquid is discussed. Based on the assumption that the shell side liquid is at the uniform and constant temperature (T_e), the methodology applied by Anand [48] is adopted in this study. Anand [49] proposed the total entropy generation ($\dot{S}_{gen}$) is
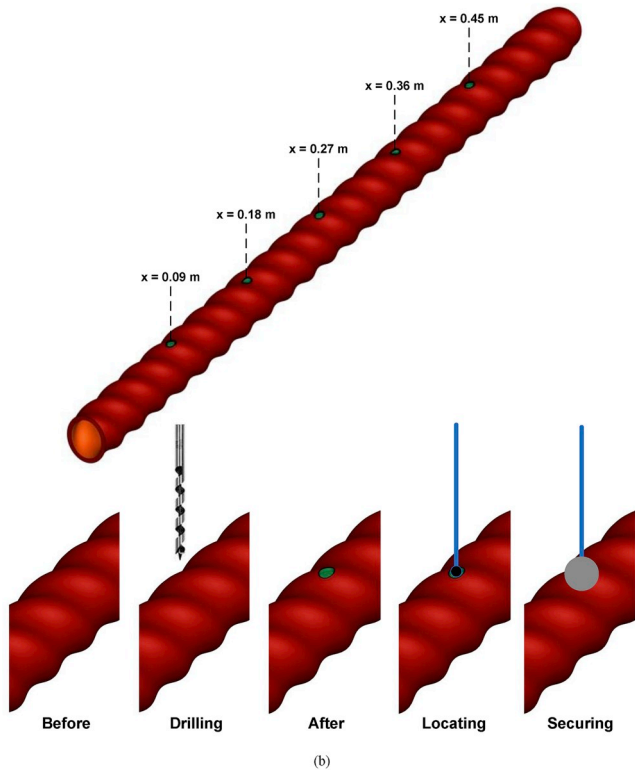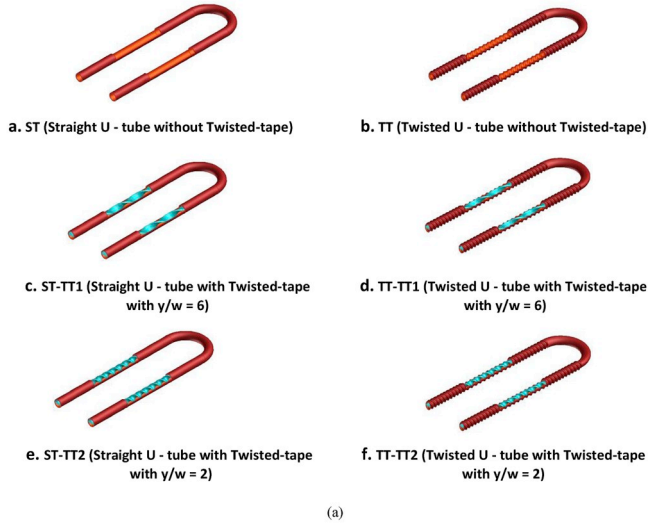
Fig. 3. (a) Layouts of twisted-tapes and U-tubes (b) Steps to install surface thermocouples.

estimated through Eq. (13). This formulation comprises entropy generated due to temperature difference and friction loss,

$$\dot{S}_{gen} = \dot{m}C_p \left[\frac{-1}{\alpha} \ln \left| \frac{1 - \tau\alpha e^{-4St\lambda_L}}{1 - \tau\alpha} \right| + \ln \left| \frac{1 - \tau e^{-4St\lambda_L}}{1 - \tau} \right| + \frac{1}{8} f\tau \frac{Ec}{St} \ln \left| \frac{e^{4St\lambda_L} - \tau}{1 - \tau} \right| \right]$$

(13)

$$\dot{S}_{gen} = \dot{S}_{gen,th} + \dot{S}_{gen,f}$$

(14)

In which, the Stanton number is computed by,

$$St = \frac{h'}{\rho u C_p}$$

(15)

Here, Eq. (16) calculates the overall heat transfer coefficient [43],

$$h' = \frac{Q_{conv}}{A_{conv}(T_e - T_b)_{LMTD}}$$

(16)

Eckert number, Ec is needed for the calculation of $\dot{S}_{gen}$ as provided in Eq. (13), which is calculated as follows,

$$Ec = \frac{u^2}{C_p(T_e - T_i)}$$

(17)

$$\alpha = 1 - \frac{Nu'}{Nu}$$

(18)

In the above relation, like Nusselt number, Nu' is computed. The length of the circular tube is non-dimensionalized as below,

$$\lambda = \frac{x}{D}$$

(19)

Also, τ is the dimensionless external fluid and tube side fluid temperature difference, expressed as follows,

$$\tau = \frac{T_e - T_i}{T_e}$$

(20)

In the literature, the entropy generation is defined in a non-dimensional entropy form. The best condition for thermal systems is attained when this parameter is minimized. In other words, entropy generation can help engineers to find the sources of irreversibilites for the reduction in value of irreversibilites in a thermal system by re-designing of geometrical parameters or operating conditions, written as follows,

$$\psi = \frac{\dot{S}_{gen}}{\dot{m}C_p}$$

(21)

In order to characterize the contribution of each irreversibility to the total entropy generation rate, an alternative irreversibility distribution parameter, called the Bejan number Be, which was defined by Paoletti et al. [50] as,

$$Be = \frac{thermal\ entropy\ generation}{total\ entropy\ generation}$$

(22)

The Bejan number varies between 0 and 1, with the entropy generated by heat transfer being dominant if Bejan number equal to 1. By contrast, when Bejan number equal to 0, the entropy generated by friction loss dominates.

The ratio of entropy generation observed with the use of augmentation techniques to the entropy generated in the primary model is called entropy generation number [51]. This relation is expressed as,

$$N_s = \frac{\dot{S}_{gen,\ a}}{\dot{S}_{gen,\ s}}$$

(23)

Heat transfer augmentation techniques with a value of N_s lower than 1 are thermodynamically desirable.

As mentioned earlier, water is used in the present study as a working fluid. During data reduction processing, all of the thermophysical properties of water are dependence on temperature. Hence, they can be calculated at T_b given by Ref. [52],

$$\rho_w = 1000 \times \left(1 - \frac{[T + 68.12963] \times [T - 3.9863]^2}{508929.2 \times [T + 68.12963]} \right)$$

(24)

$$K_w = -0.3838 + 0.005253 \times [T + 273] - 0.000006369 \times [T + 273]^2$$

(25)

$$\mu_w = \left(\exp \left[-2.10 + -4.45 \times \left(\frac{273}{T + 273} \right) + 6.55 \times \left(\frac{273}{T + 273} \right)^2 \right] \right)$$
$$\times (0.00179)$$

(26)

$$C_{pw} = \begin{bmatrix} 7.25575005 \times 10^1 - 6.62445402 \times 10^{-1} \times (T + 273) \\ + 2.56198746 \times 10^{-3} \times (T + 273)^2 - 4.36591923 \times 10^{-6} \\ \times (T + 273)^3 + 2.78178981 \times 10^{-9} \times (T + 273)^4 \end{bmatrix} \times R$$

(27)

In which, the average water temperature (T) is expressed in degree Celsius while R is known as the universal gas constant.

In this study, the error analysis is performed for the experimental results obtained, using Kline and McClintock [53] work. The uncertainties related to the experimental data are predicted based on the accuracy of each instrument and the following equation,

$$\frac{\delta R}{R} = \frac{1}{R} \left[\sum_{j=1}^{M} \left(\frac{\partial R}{\partial X_j} \delta X_j \right)^2 \right]^{0.5}$$

(28)

In which, ΔR, δX_j are the uncertainties associated with the dependent, R, and independent, X_j, variables, respectively. The details concerning the greatest uncertainty values for different instruments and essential experimental parameters are given in Tables 2 and 3, respectively. For instance, the uncertainty of Nusselt number, i.e. Eq. (5) is estimated as below,

$$\frac{\Delta Nu}{Nu} = \frac{1}{Nu} \left[\left\{ \frac{\partial Nu}{\partial h} \Delta h \right\}^2 + \left\{ \frac{\partial Nu}{\partial D_h} \Delta D_h \right\}^2 \right]^{0.5}$$
$$= \left[\left\{ \frac{\Delta h}{h} \right\}^2 + \left\{ \frac{\Delta D_h}{D_h} \right\}^2 \right]^{0.5}$$

(29)

4. Results and discussion

4.1. Experimental setup validation

To demonstrate the reliability and correctness of the experimental setup and to avoid any irregularities in data reduction methodology, the researchers initially evaluate the Nusselt number and the friction factor through performing tests on the smooth U-tube without any twisted-tape inserts (ST). Subsequently, the data obtained in the experiments are compared against the well-known empirical correlations developed by Dittus-Boelter [54] and Gnelinski [55] for Nusselt number and Petukhov [56] and Blasius [57] for friction factor.

The comparison of empirical data and experimental results for the *Nu* and *f* with respect to Re are presented in Fig. 4. According to Fig. 5, for the different ranges of Reynolds numbers, the results of the experimental investigation are congruent with the data obtained by the above correlations. The deviations percentage of the present results for the heat transfer in the smooth U-tube (*Nu*) and friction factor (*f*) from the equations are below ± 10%. Hence, the credibility of the experimental system and data reduction methodology can be confirmed.

4.2. Fluid flow and heat transfer

The influences of the twisting and twisted-tapes on the Nusselt number of the U-tube are disclosed in Fig. 6. According to Fig. 6, it is detected that the Nusselt number augments averagely by about of 22.7%–101.2% in the enhanced models relative to the ST depending on twist ratio and twisted walls. As expected, comparing between TT and

Table 3
The values of error for experimental parameters.

Parameters	Maximum uncertainty (%)
1. *Nu*	2.67
2. *f*	3.41
3. *Re*	1.72
4. S_{gen}	4.89

ST models reveals that twisting the tube walls causes an increase in the heat transfer rate. This behavior results from the swirl flows generated in a twisted tube which facilitates the disturbance of the fluid flow and intensifies the turbulence close to the wall. In the current study, the Nusselt number in the TT model compared to ST model possesses higher value of about 38.1% in average.

As the other point, Fig. 6 has shown that the using twisted-tapes through smooth and twisted U-tube (ST and TT) results in a superior heat transfer rate. For instance, at Reynolds number of 3853, the Nusselt number of the ST-TT1 model is found to be higher about 31.2% than that in ST model. This behavior is a consequence of the working fluid in the flow passage is revolved by the twisted-tapes and produce longitudinal/vertical vortexes which leads fluid can flow from the core region to the tube wall. Consequently, it results in the decrease in temperature gradient, improving heat transfer performance. In addition, from comparison of TT-TT1 model and ST-TT1 model, it is also found that with the installation of the same twisted-tapes, the TT model yields higher thermal performance relative to the ST model due to twisted-tapes intensify the swirl flows generated by twisted walls. In the studied range of Reynolds number, the Nusselt number in ST-TT1 model and TT-TT1 model is found to be higher about 22.7% and 27.9% than that compared to their original U-tube without inserts (ST model and TT model), respectively.

In addition, at a given Reynolds number, with the decrease in the twist ratio, the longer flow path and better mixing are attained, resulting in an increase in the heat transfer rate. The obtained results indicate that the heat transfer rate in the ST-TT2 model when compared to the ST-TT1 model yields higher value about 30.4% in average. As the other point, the Nusselt number of all cases increases by increasing Reynolds number. This can be explained that an increase in the velocity is responsible for the higher disturbance of the fluid flow which brings about an augmentation in the heat transfer rate. For instance, for the range of Reynolds number from 3844 to 11,436, the heat transfer rate of the TT-TT2 model is found to be higher approximately 122.4–84.7% than that in the ST model.

The plot of Fig. 7 has presented the distribution of pressure drop in term of friction factor against Reynolds number for all configurations. As depicted in Fig. 7, the enhanced models provide a larger resistance relative to the ST model. This behavior results from the obstructions caused by the insertion of twisted-tapes and twisted walls along to flow path and having more contact surface area with fluid. For instance, the friction factor in the TT and TT-TT1 models augments averagely by about of 27.8% and 53% in comparison with the ST model, respectively. It can be seen that as twist ratio decreases, a larger pressure drop is gained. It is a consequence of increasing the number of twists. In the studied range of Reynolds number, the friction factor in the TT-TT2

Table 2
The values of error for experimental instruments.

| Name of instrument	Range of instrument	Accuracy	Min. and max. values measured in experiments	Uncertainty %
Ultrasonic flow meter	Volumetric flow rate	$\pm 8.5 \times 10^{-7}\,\mathrm{m^3/s}$	0.28–$0.85\,\mathrm{m\,s^{-1}}$	0.525
T-type thermocouples	Inlet and outlet bulk temperatures	0.1 K	289.15–291.6 K	0.323
K-type thermocouples	Surface temperature	0.1 K	292.9–296.45 K	0.249
Pressure transmitters	Inlet and outlet bulk pressures	10 Pa	282-11,504 Pa	0.676
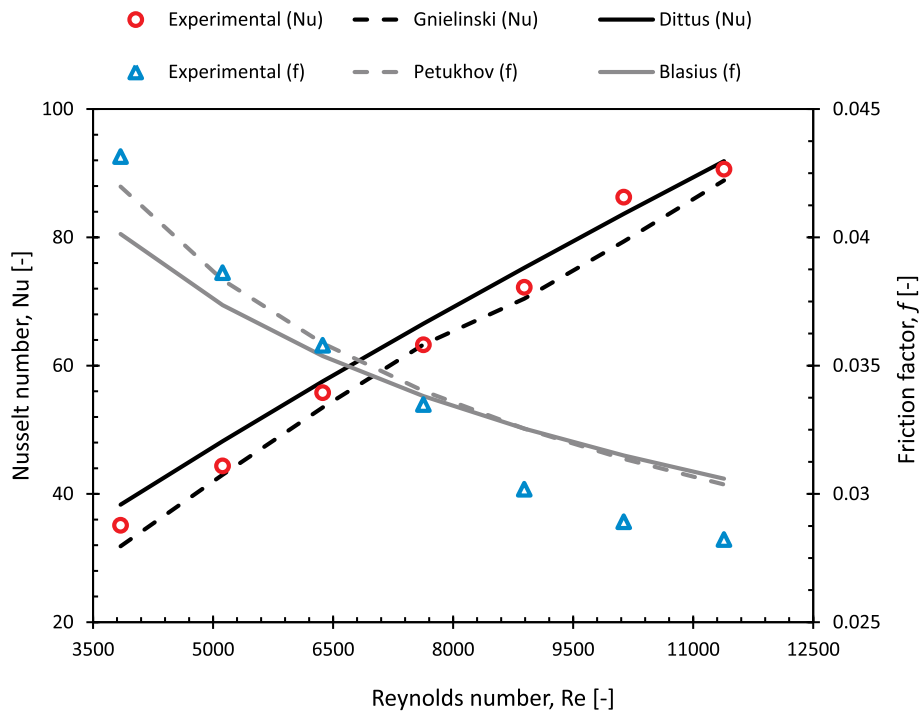
Fig. 4. Validation of experimental data obtained for the hydrothermal characteristics with correlations for ST model.

model when compared to the TT-TT1 model yields higher value about 13.6% in average. In addition, the pressure drop has descending trend when the Reynolds number goes up. In fact, as velocity increases, the turbulent intensity enhances and thus results in higher pressure drop values. The friction factor of the TT-TT2 model is found to be larger about 60.9–78.4% than that of the ST model for the range of Reynolds number from 3871 to 11,436.

To further investigate the hydrothermal characteristics, the

comparison between the overall performance of the tested twisted tube with twisted-tapes and the primary model is obligatory. Figs. 8–10 give the distribution of the Nusselt number ratio, friction factor ratio, and surface goodness factor respectively indexed by Nu_{enh}/Nu_{ST}, f_{enh}/f_{ST}, and JF.

According to Fig. 8, it is observed that the Nusselt number ratio decreases when the Reynolds number increases. Compared to the ST model, the enhanced models provide 1.31–1.12, 1.44–1.25, 1.78–1.45,
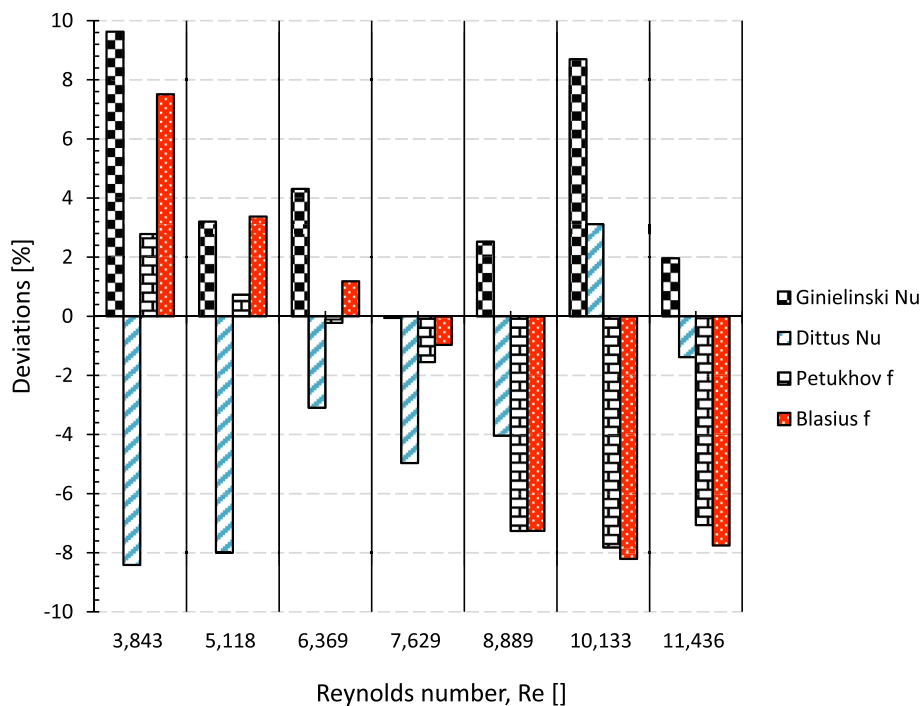

Fig. 5. Percentage deviation between current results and correlations.
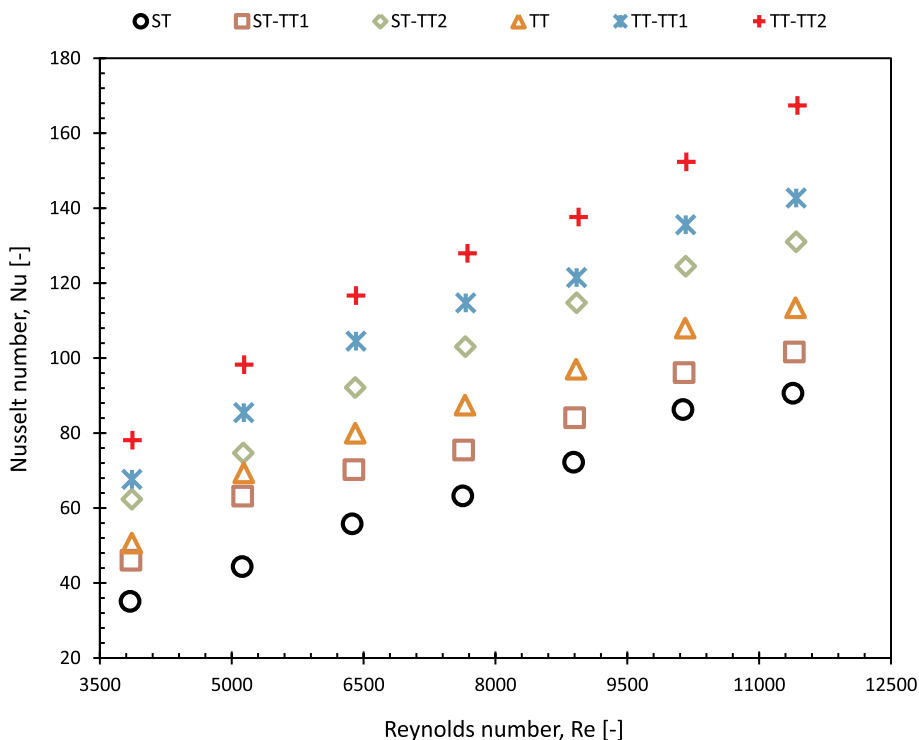
Fig. 6. The variation of the Nusselt number against Reynolds number in the range of turbulent for the simple tube and different kinds of enhanced tubes.

1.93–1.57 and 2.22–1.85 times higher of Nusselt number for ST-TT1, TT, ST-TT2, TT-TT1, and TT-TT2, respectively.

As illustrated in Fig. 9, the friction factor ratio of all enhanced models decreases with slight slope. In other words, the variation of this ratio versus Reynolds number remains somewhat constant. The friction factor in ST-TT1, TT, ST-TT2, TT-TT1, and TT-TT2 possess averagely

1.14, 1.23, 1.29, 1.42, and 1.59 times higher than the ST model, respectively.

It can be seen from Fig. 10 that the trends of the Nusselt number ratio and friction factor ratio contribute to the enhanced tubes improve the overall thermal performance especially at lower Reynolds number. Furthermore, it is obvious that the surface goodness factor for all cases
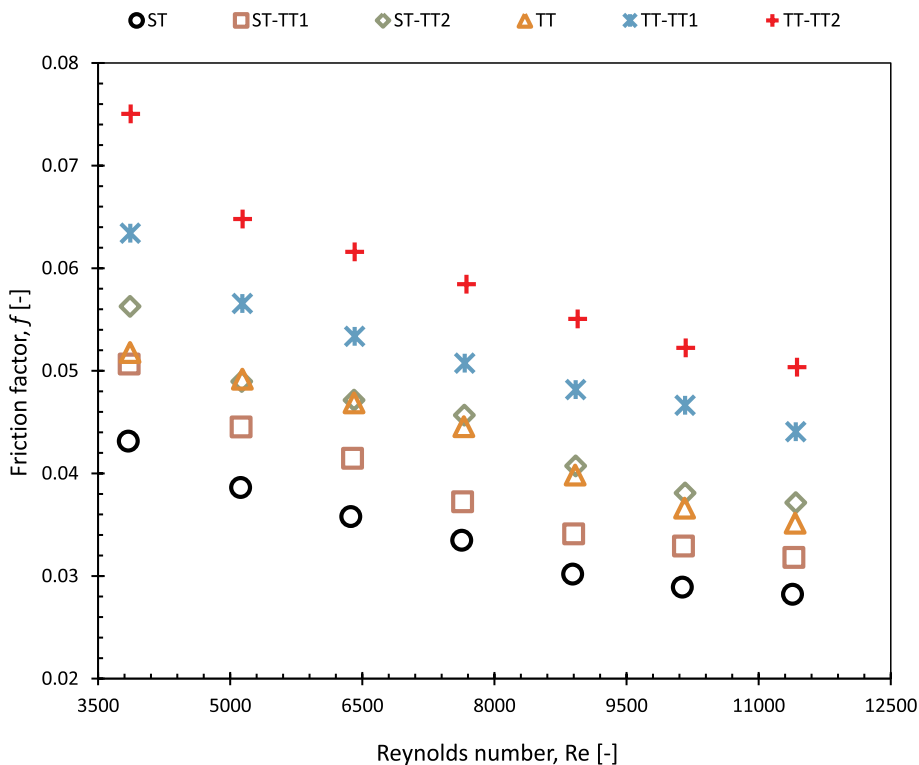

Fig. 7. The variation of the Friction factor against Reynolds number in the range of turbulent for the simple tube and different kinds of enhanced tubes.
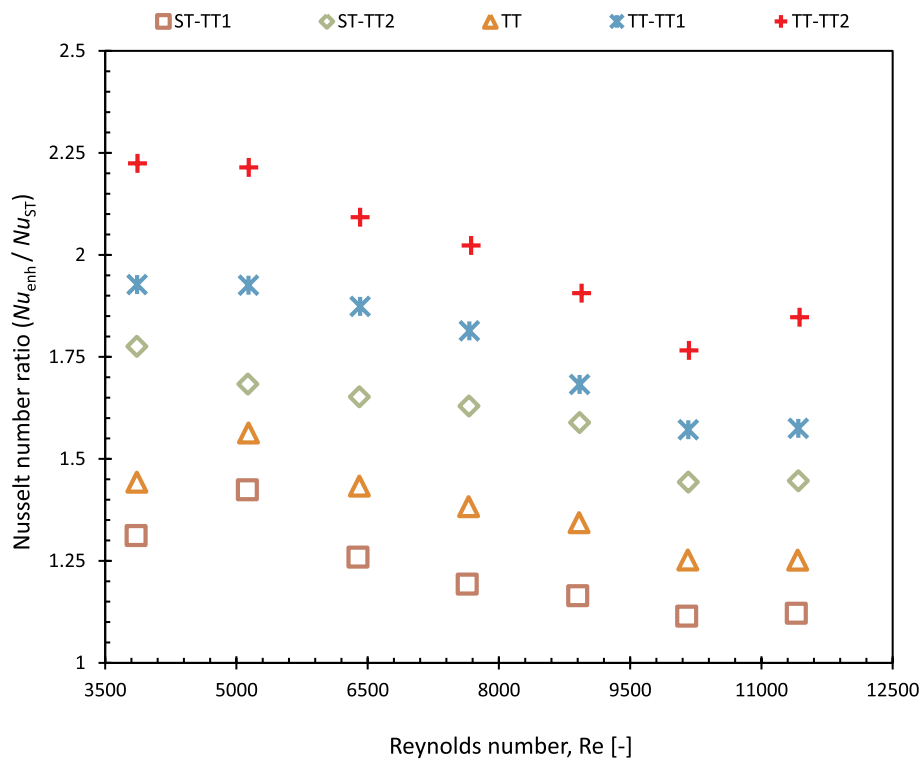
Fig. 8. Nu_{enh}/Nu_{ST} against Reynolds number in the range of turbulent for different kinds of enhanced tubes.
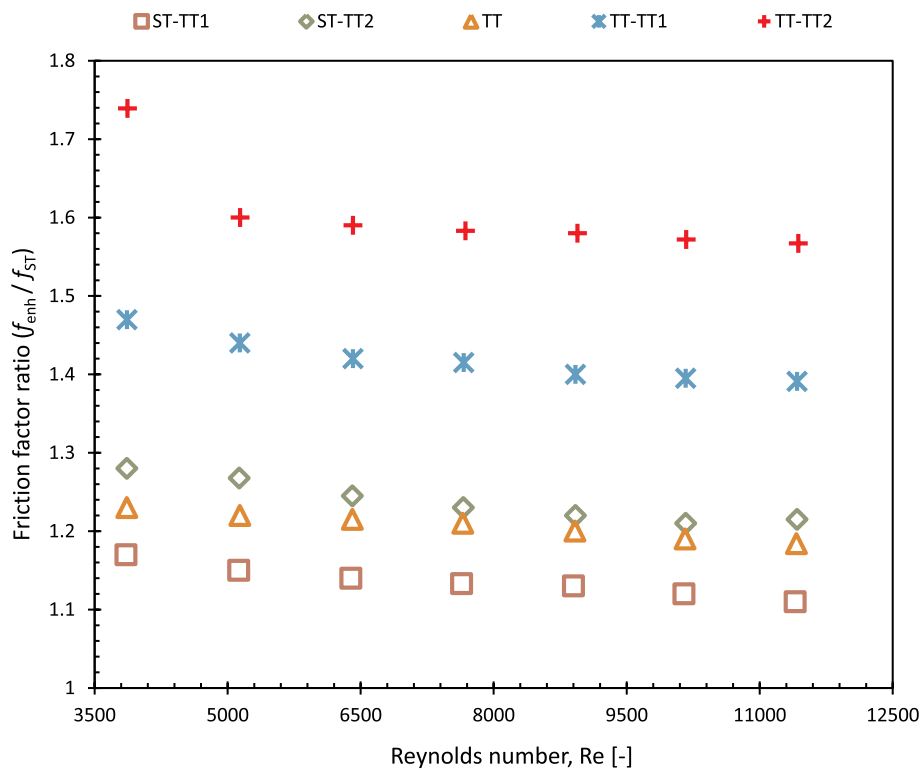

Fig. 9. f_{enh}/f_{ST} against Reynolds number in the range of turbulent for different kinds of enhanced tubes.

is higher than unity, which means that the heat transfer augmentation by the passive technologies dominates the frictional resistance. The surface goodness factor for the enhanced model reaches the highest value for the TT-TT2 model, which is about 1.89 at Reynolds number of

3871. This results from the use of twisted-tapes strengthen the secondary flows generated by twisting walls, which causes a better mixing.

A comparison between the studied models in the current work and other enhanced tubes, i.e. three-start spirally twisted tube [22], spiral
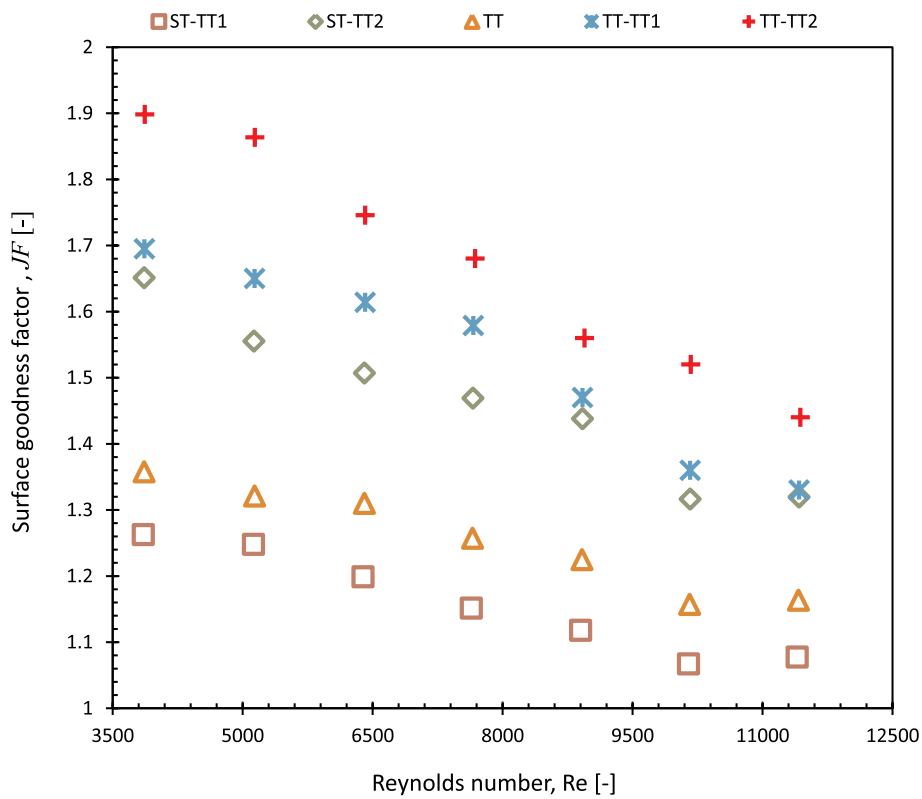
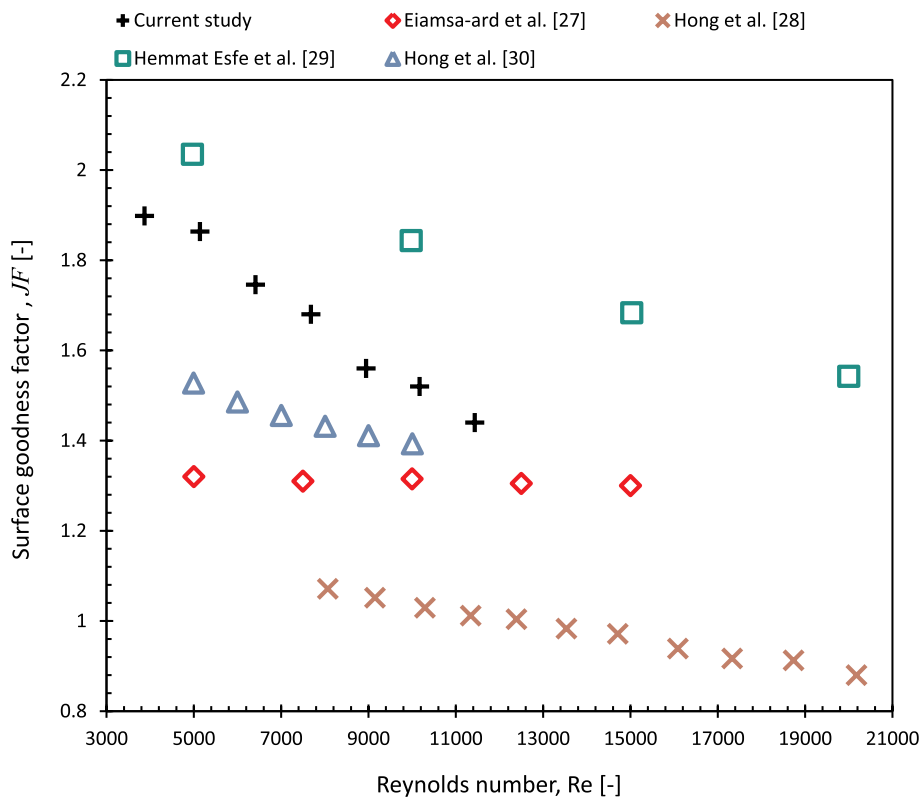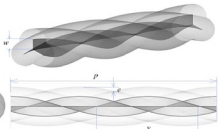**Fig. 10.** Surface goodness factor against Reynolds number in the range of turbulent for different kinds of enhanced tubes.
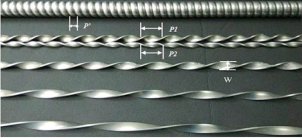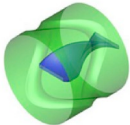

Fig. 11. Comparison surface goodness factor between present work and previous studies.

Table 4
Details of other enhanced tubes with twisted tapes.

Geometrical structure of enhanced tubes	Nu_{enh}/Nu_{ST}	f_{enh}/f_{ST}	Re	Authors
	1.95–2.05	4.3–4.7	5000–15,000	Eiamsa-ard et al. [27]
	2.31–2.77	16.9–19.5	8000–22,000	Hong et al. [28]
	1.47–2.11	2.5–4	5000–20,000	Hemmat Esfe et al. [29]
	2.54–2.66	2.2–4.3	5000–10,000	Hong et al. [30]

grooved tube [23], tri-lobed tube [24], and sinusoidal rib tube [25], using twisted tapes in terms of surface goodness factor (*JF*) under turbulent flow is presented in Fig. 11. Also, the photograph and operating condition of theses enhanced tubes are tabulated in Table 4. It can be seen from the figure that for all cases, *JF* shows descending trend with the increment in Reynolds number. From comparing three-start spirally twisted tube, spiral grooved tube, sinusoidal rib tube and current study, it is revealed that the PEC values given by the studied twisted with lower twist ratio are higher than those of Eiamsa-ard et al. [22] and Hong et al. [23,25]. As presented in Table 4, this behavior comes from lower penalty in pressure drop of this study in comparison with other cases. In other words, although the Nusselt number ratio of all case comparatively vary in a same range, other enhanced tubes relative to current study generate higher frictional resistance caused by larger surface area and blockages along tubes, resulting in the current work shows better overall hydrothermal performance. Tri-lobed tube with twisted tape have better efficiency, compared to current study. It can be attributed that the structure of this tube generates stronger swirl flow and leads to better mixture of cold fluid in core region and hot fluid in neighbor of walls.

4.3. Entropy generation analyses

Entropy generation analysis is employed to show the best parameters and operating conditions of the thermal systems by minimizing the entropy generation caused by temperature differences and friction loss. In this section, entropy generation analyses employed for various configurations are presented.

The variations of non-dimensional entropy generation through temperature differences (ψ_{th}), friction loss (ψ_f) and non-dimensional total entropy generation (ψ_t) against *Re* in all configurations are presented respectively in Fig. 12(a–c). From Fig. 12(a), it is found that rising Reynolds number is associated with a decrease in ψ_{th} for all cases. The main reason of this behavior is on account of the reduction in temperature gradient which brings about ψ_{th} reduces.

Evidently, the use of twisted-tapes leads a lower ψ_{th}. For instance, at

Reynolds number of 3853, the non-dimensional entropy generation of the ST-TT1 model reduces about 23.5% in relative to the ST model. As before stated, this is due to the formation of swirl flows, providing a better fluid mixing. Moreover, from the comparison of TT-TT1 and ST-TT1, the TT model shows lower ψ_{th} as compared to the ST model, which comes from higher thermal performance and lower temperature gradient. As aforementioned, the swirl flows induced by the twisted tubes amplify turbulence near the twisted walls, improving the heat transfer rate. In the studied range of Reynolds number, the TT-TT1 and ST-TT1 models possess lower non-dimensional entropy generation about 16.9% and 23.5% than that compared to their original U-tube without inserts (ST and TT), respectively.

In addition, the lower twist ratio offers less non-dimensional thermal entropy generation. This occurs since the enhanced tube endures a more intense path flow leading stronger mixing which diminishes ψ_{th}. For instance, the non-dimensional thermal entropy generation of the TT model equipped with twisted-tapes shows about 7.9% decrement by decreasing the twist ratio from 6 to 2 at Reynolds number of 3870.

As shown in Fig. 12(b), the enhanced tubes provide a higher ψ_f compared to the ST model. It can be explained that by the augmentation of the velocity gradient in response to more contact surface area with fluid. Among the enhanced tubes, the TT-TT2 and ST-TT1 models show the highest and lowest values of ψ_f, respectively. The values of ψ_f show an increasing trend as twist ratio value diminishes. This emanates from the increment in the number of twists which increases the velocity gradient. For instance, the non-dimensional frictional entropy generation of the TT-TT2 improve by about 17% in comparison with the TT-TT1 model.

The first observation from Fig. 12(c) is that ψ_t has a descending trend which can be explained by the fact that the decrease in ψ_{th} is larger than that of ψ_f. As can be observed in Fig. 12(a) and (b), the magnitude order of entropy generation is prominent. The frictional irreversibility is much smaller compared to the thermal irreversibility. On the other hand, Fig. 13 shows the proportion of thermal entropy generation to the total entropy generation, and the plots illustrating
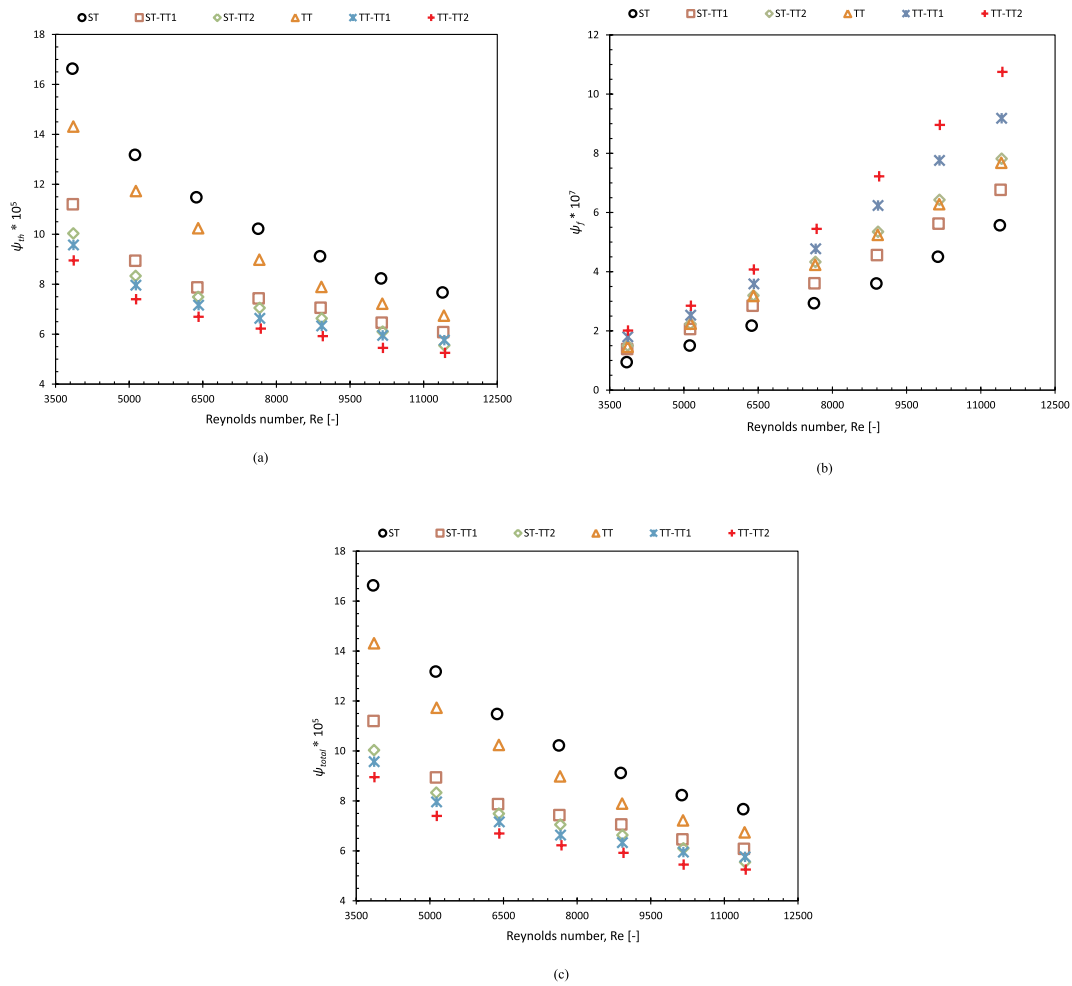
(a)

(b)

(c)

Fig. 12. The distribution of the non-dimensional entropy generation against Reynolds number in the range of turbulent for the simple tube and different kinds of enhanced tubes. (a) Thermal (ψ_{th}). (b) Friction (ψ_f). (c) Total (ψ_t).

that the Bejan number values (Be) are close to unity. In other words, the thermal entropy generation is very delicate, confirming that the tendency of ψ_t is dominated by ψ_{th} as depicted in Fig. 12(c). In addition, the least value of ψt is achieved by TT-TT2 at Reynolds number of 11,436.

According to Fig. 13, Be in all configurations decreases with increasing Re. This trend reveals that gradually friction plays a more active role at high Reynolds number, while heat transfer intensity is weakened due to the decrement of temperature gradients inside the fluid.

The variation of entropy generation number (N_s) for different kinds of the enhanced tubes against Reynolds number is summarized in Fig. 14. This figure illustrates that N_s increases with an increase in Reynolds number. So, increasing volumetric flow rate is thermodynamically disadvantageous. Also, N_s decreases with the reduction in twist ratio. As mentioned earlier, heat transfer systems will be efficient from standpoint of entropy generation, if N_s is less than unity. The range of N_s against Reynolds number changes from 0.63 to 0.91, 0.66 to 0.94, 0.69 to 1.01, 0.77 to 1.05 and 0.84 to 1.09, for TT-TT2, TT-TT1, ST-TT2, ST-TT1, and TT, respectively. As depicted in Fig. 14, the use of twisted-tapes in U-tube is beneficial from viewpoint of entropy generation for Reynolds number lower than about 8950. Based on the data of present investigation, the twisted U-tube with twisted-tapes is thermodynamically helpful for all Reynolds numbers and is recommended because illustrates the lower irreversibility relative to the other enhanced tubes.

5. Conclusion

Here, hydrothermal characteristics and entropy generation rate are examined for fully developed turbulent flows inside the twisted U-tube using twisted-tape inserts. The investigation is performed under isothermal external fluid conditions for Reynolds numbers ranging from 3843 to 11,436. The influences of different twisted-tapes and tube sides are explored. The main results of the present experimental study are revealed as follow:

- The use of the ST and TT with twisted-tapes yields higher friction factor and Nusselt number values than using the tubes without the twisted-tapes.
- In the case of twisted tube with twisted-tape, the Nusselt number and friction factor of TT-TT2 possesses 2.03 and 1.59 higher times than the ST model.
- For all cases, the surface goodness factor (JF) decreases as Reynolds number is increases, which means that the enhanced tubes have better hydrothermal performance at lower Reynolds number.
- The highest value of surface goodness factor is recorded about 1.89 for the TT-TT2 model at $Re = 3871$
- The use of twisted-tapes with lower ratio is strongly recommended because the decrement in twist ratio decreases thermal entropy generation, while frictional entropy generation increases. Owing to the superiority of thermal entropy generation, the total entropy generation reduces.
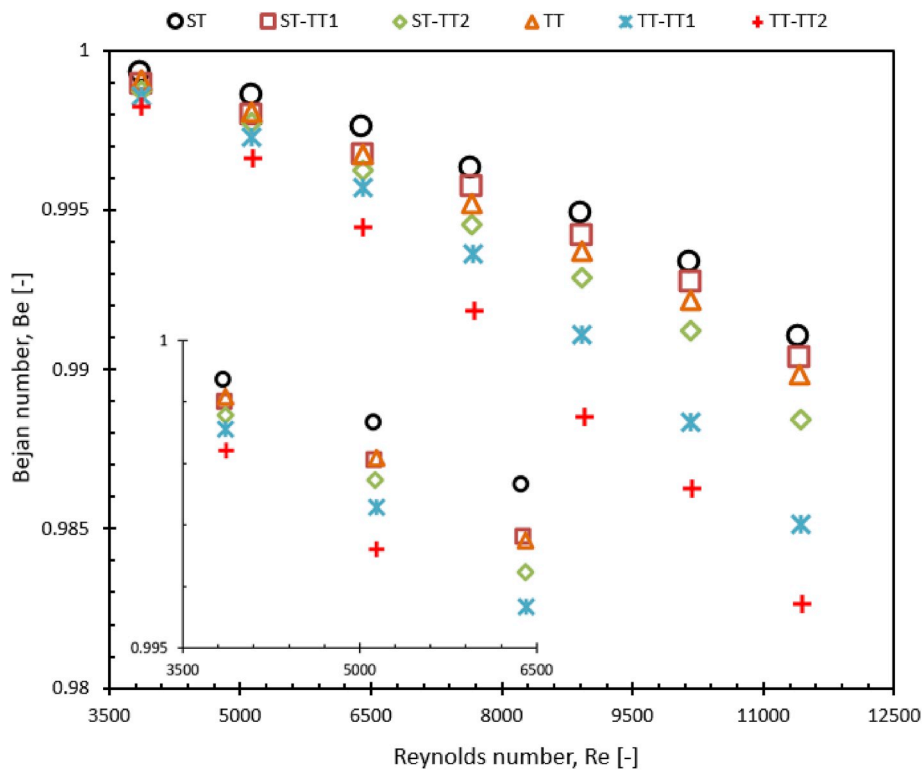
Fig. 13. Bejan number against Reynolds number for the simple tube and different kinds of enhanced tubes.
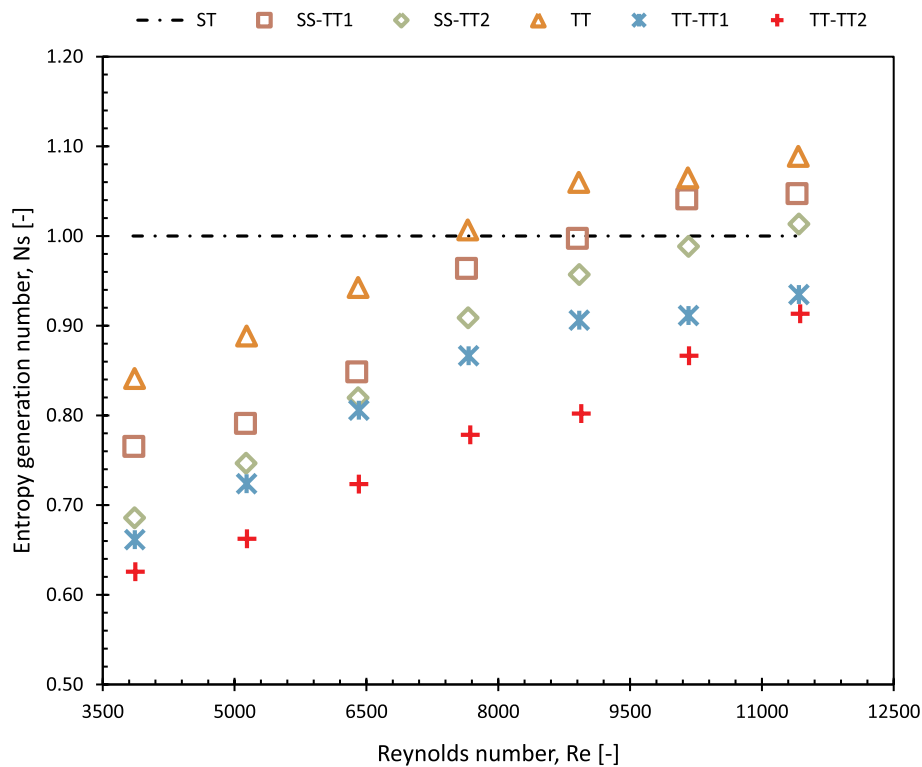
Fig. 14. The variation of entropy generation number against Reynolds number for the simple tube and different kinds of enhanced tubes.

- The non-dimensional thermal entropy generation of TT model with twisted tapes indicates 7.9% reduction as the twist ratio is decreased from 6 to 2 at Reynolds number of 3870.
- Entropy generation rate is reduced considerably at low Reynolds numbers. Also, entropy generation analysis revealed that ST-TT1 and ST-TT2 are thermodynamically advantageous for Reynolds numbers up to 8950 while TT-TT1 and TT-TT2 are advantageous for all studied Reynolds number.

Conflicts of interest

None declared.

Acknowledgements

Nomenclature

A	Area of tube side, m^2
A_c	Axial flow cross-sectional area, m^2
C_p	Specific heat capacity, $J\,kg^{-1}\,K^{-1}$
D	Inner diameter, m
D_h	Hydraulic diameter, m
h	Internal heat transfer coefficient, $W\,m^{-2}\,K^{-1}$
h'	Overall heat transfer coefficient, $W\,m^{-2}\,K^{-1}$
JF	Surface goodness factor $(-)$
l	U-tube length, m
p	Pressure, Pa
P_w	Wetted perimeter, m
Q	Heat transfer rate, W
T	Temperature, K
$\dot{S}$	Entropy generation rate, $W\,K^{-1}$
u	Velocity, $m\,s^{-1}$
V	Volumetric flow rate, $m^3\,s^{-1}$

Greek symbols

α	non-dimensional parameter
τ	non-dimensional temperature difference
λ	non-dimensional tube side length
λ_L	non-dimensional tube side length at x = L
Ψ	non-dimensional entropy generation rate
Δp	Pressure drop, Pa
κ	Thermal conductivity, $W\,m^{-1}\,K^{-1}$
μ	Dynamic viscosity, $kg\,m^{-1}\,s^{-1}$
ρ	Density, $kg\,m^{-3}$

Subscripts

b	Bulk
$conv$	Convection
e	External
f	Fluid
in	Inlet
out	Outlet
w	Wall
wi	Local

Dimensionless groups

Ec	Eckert number
f	Friction factor
N_s	Entropy generation number
Nu	Internal Nusselt number
Nu'	Overall Nusselt number
Re	Reynolds number
St	Stanton number

Acronyms

S_T	straight U-tube without twisted-tapes
ST-TT1	straight U-tube with twisted-tapes with higher ratio
ST-TT2	straight U-tube with twisted-tapes with lower ratio
TT	twisted U-tube without twisted-tapes
TT-TT1	twisted U-tube with twisted-tapes with higher ratio
TT-TT2	twisted U-tube with twisted-tapes with lower ratio

References

[1] S. Eiamsa-Ard, C. Thianpong, P. Eiamsa-Ard, P. Promvonge, Convective heat transfer in a circular tube with short-length twisted tape insert, Int. Commun. Heat Mass Transf. 36 (2009) 365–371.

[2] W.H. Azmi, K.V. Sharma, P.K. Sarma, R. Mamat, S. Anuar, Comparison of convective heat transfer coefficient and friction factor of TiO₂ nanofluid flow in a tube with twisted tape inserts, Int. J. Therm. Sci. 81 (2014) 84–93.

[3] A.E. Bergles, ExHFT for fourth generation heat transfer technology, Exp. Therm. Fluid Sci. 26 (2002) 335–344.

[4] W. Liu, Z. Liu, T. Ming, Z. Guo, Physical quantity synergy in laminar flow field and its application in heat transfer enhancement, Int. J. Heat Mass Transf. 52 (2009) 4669–4672.

[5] W. Liu, Z.C. Liu, S.Y. Huang, Physical quantity synergy in the field of turbulent heat transfer and its analysis for heat transfer enhancement, Chin. Sci. Bull. 55 (2010) 2589–2597.

[6] W. Liu, Z.C. Liu, H. Jia, A.W. Fan, A. Nakayama, Entransy expression of the second law of thermodynamics and its application to optimization in heat transfer process, Int. J. Heat Mass Transf. 54 (2011) 3049–3059.

[7] M. Ebrahimi Dehshali, S.Z. Najm Barzanji, A. Hakkaki-Fard, Pool boiling heat transfer enhancement by twisted-tape fins, Appl. Therm. Eng. 135 (2018) 170–177.

[8] Y. He, L. Liu, P. Li, L. Ma, Experimental study on heat transfer enhancement characteristics of tube with cross hollow twisted tape inserts, Appl. Therm. Eng. 131 (2018) 743–749.

[9] S. Eiamsa-Ard, C. Thianpong, P. Eiamsa-Ard, Turbulent heat transfer enhancement by counter/co-swirling flow in a tube fitted with twin twisted tapes, Exp. Therm. Fluid Sci. 34 (2010) 53–62.

[10] S.M. Abolarin, M. Everts, J.P. Meyer, Heat transfer and pressure drop characteristics of alternating clockwise and counter clockwise twisted tape inserts in the transitional flow regime, Int. J. Heat Mass Transf. 133 (2019) 203–217.

[11] S. Eiamsa-ard, K. Kiatkittipong, Heat transfer enhancement by multiple twisted tape inserts and TiO₂/water nanofluid, Appl. Therm. Eng. 70 (2014) 896–924.

[12] J. Guo, A. Fan, X. Zhang, W. Liu, A numerical study on heat transfer and friction factor characteristics of laminar flow in a circular tube fitted with center-cleared twisted tape, Int. J. Therm. Sci. 50 (2011) 1263–1270.

[13] X. Zhang, Z. Liu, W. Liu, Numerical studies on heat transfer and flow characteristics for laminar flow in a tube with multiple regularly spaced twisted tapes, Int. J. Therm. Sci. 58 (2012) 157–167.

[14] C. Thianponga, P. Eiamsa-arda, P. Promvongea, S. Eiamsa-ard, Effect of perforated twisted-tapes with parallel wings on heat transfer enhancement in a heat exchanger tube, Energy Procedia 14 (2012) 1117–1123.

[15] C. Qi, M. Liu, T. Luo, Y. Pan, Z. Rao, Effects of twisted tape structures on thermo-hydraulic performances of nanofluids in a triangular tube, Int. J. Heat Mass Transf. 127 (2018) 146–159.

[16] J.P. Meyer, S.M. Abolarin, Heat transfer and pressure drop in the transitional flow regime for a smooth circular tube with twisted tape inserts and a square-edged inlet, Int. J. Heat Mass Transf. 117 (2018) 11–29.

[17] M. Khoshvaght-Aliabadi, S. Davoudi, M.H. Dibaei, Performance of agitated-vessel U tube heat exchanger using spiky twisted tapes and water based metallic nanofluids, Chem. Eng. Res. Des. 133 (2018) 26–39.

[18] N.T.R. Kumara, P. Bhramaraa, A. Kirubeilb, L.S. Sundarc, M.K. Singhc, A.C.M. Sousa, Effect of twisted tape inserts on heat transfer, friction factor of Fe₃O₄ nanofluids flow in a double pipe U-bend heat exchanger, Int. Commun. Heat Mass Transf. 95 (2018) 53–62.

[19] L. Zhang, S. Yang, H. Xu, Experimental study on condensation heat transfer characteristics of steam on horizontal twisted elliptical tubes, Appl. Energy 97 (2012) 881–887.

[20] R. Bhadouriya, A. Agrawal, S.V. Prabhu, Experimental and numerical study of fluid flow and heat transfer in an annulus of inner twisted square duct and outer circular pipe, Int. J. Therm. Sci. 94 (2015) 96–109.

[21] X. Tang, X. Dai, D. Zhu, Experimental and numerical investigation of convective heat transfer and fluid flow in twisted spiral tube, Int. J. Heat Mass Transf. 90 (2015) 523–541.

[22] M. Khoshvaght-Aliabadi, Z. Arani-Lahtari, Forced convection in twisted mini-channel (TMC) with different cross section shapes: a numerical study, Appl. Therm. Eng. 93 (2016) 101–112.

[23] J. Cheng, Z. Qian, Q. Wang, Analysis of heat transfer and flow resistance of twisted oval tube in low Reynolds number flow, Int. J. Heat Mass Transf. 109 (2017) 761–777.

[24] W. Yan, X. Gao, X. Xu, C. Ding, Z. Zhang, Heat transfer performance of epoxy resin Flows in a horizontal twisted tube, Appl. Therm. Eng. 127 (2017) 28–34.

[25] A. Feizabadi, M. Khoshvaght-Aliabadi, A.B. Rahimi, Numerical investigation on Al₂O₃/water nanofluid flow through twisted-serpentine tube with empirical validation, Appl. Therm. Eng. 137 (2018) 296–309.

[26] M. Khoshvaght-Aliabadi, A. Feizabadi, S.F. Khaligh, Empirical and numerical assessments on corrugated and twisted channels as two enhanced geometries, Int. J. Mech. Sci. 157 (2019) 25–44.

[27] S. Eiamsa-ard, P. Promthaisong, C. Thianpong, M. Pimsarn, V. Chuwattanakul, Influence of three-start spirally twisted tube combined with triple-channel twisted tape insert on heat transfer enhancement, Chem. Eng. Process Process Intensif. 102 (2016) 117–129.

[28] Y. Hong, J. Du, S. Wang, Experimental heat transfer and flow characteristics in a spiral grooved tube with overlapped large/small twin twisted tapes, Int. J. Heat Mass Transf. 106 (2017) 1178–1190.

[29] M. Hemmat Esfe, H. Mazaheri, S.J. Mirzaei, E. Kashi, M. Kazemi, M. Afrand, Effects

of twisted tapes on thermal performance of tri-lobed tube: an applicable numerical study, Appl. Therm. Eng. 144 (2018) 512–521.

[30] Y. Hong, J. Du, Q. Li, T. Xu, W. Li, Thermal-hydraulic performances in multiple twisted tapes inserted sinusoidal rib tube heat exchangers for exhaust gas heat recovery applications, Energy Convers. Manag. 185 (2019) 271–290.

[31] A. Bejan, Thermodynamic optimization of geometry in engineering flow systems, Exergy, Int. J. 1 (2001) 269–277.

[32] A. Bejan, third ed., Mechanical Engineers Handbook Energy and Power vol. 4, John Wiley & Sons, 2006.

[33] N. Zheng, P. Liu, F. Shan, Z. Liu, W. Liu, Turbulent flow and heat transfer enhancement in a heat exchanger tube fitted with novel discrete inclined grooves, Int. J. Therm. Sci. 111 (2017) 289–300.

[34] I. Kotcioglu, S. Caliskan, A. Cansiz, S. Baskaya, Second law analysis and heat transfer in a cross-flow heat exchanger with a new winglet-type vortex generator, Energy 35 (2010) 3686–3695.

[35] O. Keklikcioglu, V. Ozceyhan, Entropy generation analysis for a circular tube with equilateral triangle cross sectioned coiled-wire inserts, Energy 139 (2017) 65–75.

[36] V. Zimparov, Enhancement of heat transfer by a combination of three start spirally corrugated tubes with a twisted tape, Int. J. Heat Mass Transf. 44 (2001) 551–574.

[37] M. Sheikholeslami, M. Jafaryar, D.D. Ganji, Z. Li, Exergy loss analysis for nanofluid forced convection heat transfer in a pipe with modified turbulators, J. Mol. Liq. 262 (2018) 104–110.

[38] S. Rashidi, N. Moghadas Zade, J.A. Esfahani, Thermo-fluid performance and entropy generation analysis for a new eccentric helical screw tape insert in a 3D tube, Chem. Eng. Process Process Intensif. 117 (2017) 27–37.

[39] M. Sheikholeslami, M. Jafaryar, Z. Li, Second law analysis for nanofluid turbulent flow inside a circular duct in presence of twisted tape turbulators, J. Mol. Liq. 263 (2018) 489–500.

[40] Z. Li, M. Sheikholeslami, M. Jafaryar, A. Shafee, A.J. Chamkha, Investigation of nanofluid entropy generation in a heat exchanger with helical twisted tapes, J. Mol. Liq. 266 (2018) 797–805.

[41] A. Mwesigye, T. Bello-Ochende, J.P. Meyer, Heat transfer and entropy generation in a parabolic trough receiver with wall-detached twisted tape inserts, Int. J. Therm. Sci. 99 (2016) 238–257.

[42] Y. Hong, J. Du, S. Wang, Turbulent thermal, fluid flow and thermodynamic characteristics in a plain tube fitted with overlapped multiple twisted tapes, Int. J. Heat

Mass Transf. 115 (2017) 551–565.

[43] M. Bahiraei, N. Mazaheri, F. Aliee, Second law analysis of a hybrid nanofluid in tubes equipped with double twisted tape inserts, Powder Technol. 345 (2019) 692–703.

[44] M. Khoshvaght-Aliabadi, M. Nouri, O. Sartipzadeh, M. Salami, Performance of agitated serpentine heat exchanger using metallic nanofluids, Chem. Eng. Res. Des. 109 (2016) 53–64.

[45] M. Farnam, M. Khoshvaght-Aliabadi, M.J. Asadollahzadeh, Heat transfer intensification of agitated U-tube heat exchanger using twisted-tube and twisted-tape as passive techniques, Chem. Eng. Process. Process Intensif. 133 (2018) 137–147.

[46] M.W. Kays, A.L. London, Compact Heat Exchangers, third ed., Kreiger Publishing, Melbourne, 1984.

[47] R.L. Webb, Performance evaluation criteria for use of enhanced heat transfer surfaces in heat exchanger design, Int. J. Heat Mass Transf. 24 (1981) 715–726.

[48] V. Anand, Entropy generation analysis of laminar flow of a nanofluid in a circular tube immersed in an isothermal external fluid, Energy Part 1 (93) (2015) 154–164.

[49] E.M. Sparrow, S.V. Patankar, Relationships among boundary conditions and nusselt numbers for thermally developed duct flows, J. Heat Transf. 99 (1977) 483–485.

[50] S. Paoletti, F. Rispoli, E. Sciubba, Calculation of Exergetic Losses in Compact Heat Exchanger Passages, (1989) Tech. Rep. ASME AES– 10.

[51] V.D. Zimparov, N.L. Vulchanov, Performance evaluation criteria for enhanced heat transfer surfaces, Int. J. Heat Mass Transf. 37 (1994) 1807–1816.

[52] S. Jarungthammachote, Entropy generation analysis for fully developed laminar convection in hexagonal duct subjected to constant heat flux, Energy 35 (2010) 5374–5379.

[53] S.J. Kline, F.A. McClintock, Describing uncertainties in single sample experiments, Mech. Eng. 75 (1953) 3–8.

[54] F.W. Dittus, L.M.K. Boelter, Heat transfer in automobile radiators of the tubular type, Int. Commun. Heat Mass Transf. 12 (1985) 3–22.

[55] V. Gnielinski, New equations for heat and mass transfer in turbulent pipe flow and channel flow, Int. Chem. Eng. 16 (1976) 359–368.

[56] B. Petukhov, Heat transfer in turbulent pipe flow with variable physical properties, in: J.P. Harnett (Ed.), Advances in Heat Transfer, vol. 6, Academic Press, New York, 1970, pp. 504–564.

[57] H. Blasius, Grenzschichten in Flussigkeiten mit kleiner Reibung (German), Z. Angew. Math. Phys. 56 (1908) 1–37.